Effect of Oily Additives on Foamability and Foam Stability. 1. Role of Interfacial Properties

ARTICLE *in* LANGMUIR · SEPTEMBER 2001

Impact Factor: 4.46 · DOI: 10.1021/la010600r

6 AUTHORS, INCLUDING:

Luben N Arnaudov
Unilever
31 PUBLICATIONS **584** CITATIONS
SEE PROFILE

Nikolai D. Denkov
Sofia University "St. Kliment Ohridski"
151 PUBLICATIONS **5,913** CITATIONS
SEE PROFILE

Effect of Oily Additives on Foamability and Foam Stability. 1. Role of Interfacial Properties

Luben Arnaudov,[†] Nikolai D. Denkov,*[,†] Irena Surcheva,[†] Patrick Durbut,[‡] Guy Broze,[‡] and Ammanuel Mehreteab[§]

Laboratory of Chemical Physics Engineering (Formerly Laboratory of Thermodynamics and Physicochemical Hydrodynamics), Faculty of Chemistry, Sofia University, 1 James Bourchier Avenue, 1164 Sofia, Bulgaria, Colgate-Palmolive Research & Development, Inc., Avenue Du Parc Industriel, B-4041 Milmort (Herstal), Belgium, and Colgate-Palmolive Technology Center, 909 River Road, Piscataway, New Jersey 08854-5596

Received April 24, 2001. In Final Form: July 23, 2001

Foam tests and model experiments with sodium dodecylbenzenesulfonate solutions are performed to clarify how the foam stability and the foaminess are affected by several oils of different chemical structure. The foam tests show that 2-butyloctanol (2BO, branched alkanol) and isohexyl-neopentanoate (IHNP, branched ester) exhibit a significant antifoam activity at concentrations as low as 0.005 wt %. *n*-Heptanol also acts as an antifoam, but at concentrations above 0.15 wt % due to its higher solubility in the surfactant solution. The model experiments prove that the antifoam activity of pre-emulsified oils is determined primarily by the barrier to drop entry, which controls the drop emergence on the solution surface. If the entry barrier is high (e.g., *n*-dodecanol and silicone oil), the oil drops remain arrested in the Plateau borders during the process of foam drainage, without being able to destroy the foam. Thus branched long-chain alkanols (like 2BO) and esters (IHNP) behave as active antifoams, because they combine the advantages of long-chain and medium-chain *n*-alkanols—low solubility and low entry barrier, respectively. No direct correlation between the spreading behavior of the oils and their foam breaking activity is observed. The effect of these oils on the foamability of the solutions is far more complex. At low concentrations (below and around their solubility limit) the oils reduce the dynamic surface tension of the solutions, facilitating in this way the formation of fresh surface and enhancing the foamability. At higher oil concentrations, however, the emulsified oil drops induce a coalescence of the foam bubbles during foaming and, as a result, the foamability of the solutions decreases. That is why the foamability is a nonmonotonic function of the oil concentration.

1. Introduction

Two important characteristics of the surfactant solutions are their foamability (foam produced by agitation) and foam stability (foam remaining after a certain period at rest), which determine the applications in areas such as personal and house-hold care, washing, food industry, fire fighting, ore flotation, and many others.[1−4] Different additives, often called foam boosters, are used to improve the foaming properties of surfactant solutions.[5,6] In other systems, additives are applied to prevent the formation of an excessive foam and are termed antifoams.[2−4,7−12]

It has been established that normal linear alkanols (*n*-alkanols) affect strongly the stability of foams produced from surfactant solutions. Kruglyakov and coauthors,[11−13] systematically studied the effect of *n*-alkanol chain length on the stability of foams produced by several surfactants: sodium dodecyl sulfate (SDS); sodium dodecylbenzenesulfonate (SDDBS); nonylphenyl polyoxyethylene-10; saponin. With all these systems, they found an optimum chain length of the alkanol that corresponded to most pronounced antifoam effect. At very low surfactant concentrations, long-chain alkanols (*n*-decanol, *n*-undecanol) were most efficient as foam breakers. At higher surfactant concentrations, typical for most applications, the medium-chain alkanols (*n*-hexanol to *n*-octanol) were more efficient. These results were explained[11−13] by two competitive effects: (i) gradual decline in the alkanol solubility and (ii) decrease of the oil polarity, with the alkanol chain length. The solubility is important, because the antifoam effect is observed at alkanol concentrations above the solubility limit, when dispersed oily drops appear in the working solutions (see Figure 1). Therefore, at low surfactant concentrations more efficient as an antifoam would be an alkanol of lower solubility which gives

* To whom correspondence may be addressed. Phone: (+359) 2−962 5310. Fax: (+359) 2−962 5643. E-mail: ND@LTPH.BOL.BG.

† Laboratory of Chemical Physics Engineering, Sofia University.

‡ Colgate-Palmolive Research & Development, Inc., Milmort (Herstal).

§ Colgate-Palmolive Technology Center, Piscataway.

(1) Prud'homme, R. K., Khan, S. A., Eds. *Foams*: *Theory, Measurements, and Applications*; Surfactant Science Series; Marcel Dekker: New York, 1996; Vol. 57.

(2) Exerowa, D.; Kruglyakov, P. M. *Foams and Foam Films*; Elsevier: Amsterdam, 1998.

(3) Pugh, R. J. *Adv. Colloid Interface Sci.* **1996**, *64*, 67.

(4) Zocchi, G. In *Handbook of Detergents*, *Part A*: *Properties*; Broze, G., Ed.; Surfactant Science Series; Marcel Dekker: New York, 1999; Vol. 82, Chapter 10.

(5) Lomax, E. G., Ed. *Amphoteric Surfactants*; Surfactant Science Series; Marcel Dekker: New York, 1996; Vol. 59.

(6) Basheva, E.; Ganchev, D.; Denkov, N. D.; Kasuga, K.; Satoh, N.; Tsujii, K. *Langmuir* **2000**, *16*, 1000. Basheva, E.; Stoyanov, S.; Denkov, N. D.; Kasuga, K.; Satoh, N.; Tsujii, K. *Langmuir* **2001**, *17*, 969.

(7) Garrett, P. R. In *Defoaming*: *Theory and Industrial Applications*; Garrett, P. R., Ed.; Surfactant Science Series; Marcel Dekker: New York, 1993; Vol. 45, Chapter 1.

(8) Aveyard, R.; Binks, B. P.; Fletcher, P. D. I.; Peck, T. G.; Rutherford, C. E. *Adv. Colloid Interface Sci.* **1994**, *48*, 93.

(9) Wasan, D. T.; Christiano, S. P. In *Handbook of Surface and Colloid Chemistry*; Birdi, K. S., Ed.; CRC Press: Boca Raton, FL, 1997; Chapter 6. Koczo, K.; Koczone, J. K.; Wasan, D. T. *J. Colloid Interface Sci.* **1994**, *166*, 225.

(10) Denkov, N. D.; Cooper, P.; Martin, J.-Y. *Langmuir* **1999**, *15*, 8514. Denkov, N. D. *Langmuir* **1999**, *15*, 8530.

(11) Kruglyakov, P. M. In *Thin Liquid Films*: *Fundamentals and Applications*; Surfactant Science Series; Ivanov, I. B., Ed.; Marcel Dekker: New York, 1988; Vol. 29, Chapter 11.

(12) Chapter 9 in ref 2.

(13) Kruglyakov, P. M.; Koretskaya, T. A. *Kolloid. Zh.* **1974**, *36*, 682.

10.1021/la010600r CCC: $20.00
Published on Web 09/29/2001

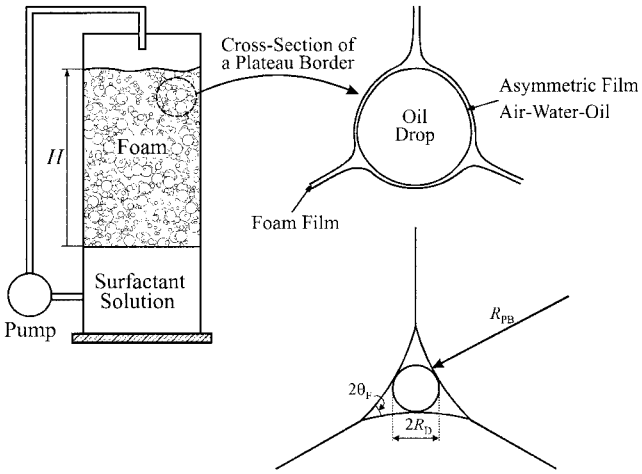

Figure 1. Mechanism of foam destruction by oil drops.[6,9] The drops are expelled from the foam films into the neighboring Plateau borders in the early stages of foam evolution. The liquid drainage leads to a gradual narrowing of the Plateau borders and to an increase of the capillary pressure compressing the trapped drops. When the compressing capillary pressure exceeds a certain critical value, which depends on the stability of the asymmetric oil−water−air film, the oil drops enter the surface of the Plateau border and rupture the neighboring foam films (the detailed mechanism of film rupture is still unclear). The oil drop radius should be larger than the radius of the inscribed sphere (i.e., than the minimal radius of a trapped drop), R_D, which depends on the foam height, H. R_{PB} is the radius of curvature of the Plateau border wall and $2\theta_F$ is the contact angle foam film meniscus.

numerous oily drops. However, at high surfactant concentration (around and above the critical micelle concentration, cmc) the adsorption layers formed at the alkanol−water interface are possibly denser for long-chain alkanols, because the latter are less polar than the short-chain alkanols. Kruglyakov and coauthors[11−13] hypothesize that these dense adsorption layers stabilize the asymmetric oil−water−air films against rupture (Figure 1), which makes the long-chain *n*-alkanols inefficient foam breakers. The effect of *n*-alkanols on the foamability was not studied by these authors.

Abe and Matsumura[14] studied the effect of alkanols and alkanediols on the foamability of SDDBS solutions. They found that lower dynamic surface tension (DST) corresponded to lower foamability of the solutions containing *n*-alkanols and concluded that *n*-octanol should be most efficient as an antifoam. Their explanation was that additives, which are able to reduce rapidly the surface tension, would eliminate the surface tension gradient (the Marangoni effect). The latter is considered to be among the major factors ensuring the stability of the foam films during their drainage.[7,15−19] However, no correlation between DST and foamability was found for alkanediols, and the effect of the additives on the foam stability was not explored at all (see also the comments in section III.C of ref 7). The possibility that the oily drops or lenses, floating on the air−water interface, could destroy the foam films by the mechanisms discussed in refs 6−13 was neglected, which makes the explanations in ref 14 incomplete.

Interestingly, in other studies the fast reduction of the surface tension is considered to be the main factor for the increased foamability of SDS solutions in the presence of long-chain alkanols, that is, the same factor is used to explain the opposite effect. For example, Patist et al.[20] introduced *n*-dodecanol in SDS solutions at a molar ratio of 1:20, when the additive is entirely solubilized within the surfactant micelles and no foam destruction by oily drops occurs. In these experiments lower DST corresponded to better foamability of the solutions. This result was explained by a simple relation implying that the energy introduced during foaming, W, is proportional to the surface tension, σ_{AW}, and the change in the surface area, ΔA: $W \propto \sigma_{AW} \Delta A$, that is, the lower dynamic surface tension enhances the foamability of the solutions. Other studies[21−25] show that the incorporation of *n*-dodecanol leads to dense and "rigid" mixed adsorption layers with SDS, which decelerate the foam film thinning and stabilize the foams.

The results described above suggest that *branched, nonlinear long-chain alkanols* (or other amphiphiles of similar chemical structure) might have interesting and useful properties as additives to foaming solutions. The low polarity of these substances ensures their low solubility in water, while the branched hydrocarbon chains could preclude the formation of dense mixed adsorption layers with the molecules of the main surfactant. Therefore, one may expect that these oils might be efficient antifoams at a relatively low concentration, because they combine the beneficial features of the medium-chain and the long-chain linear *n*-alkanols. It is impossible to predict in advance what would be the effect of the branched long-chain alkanols on the foamability of the solutions.

To check the above ideas, we performed a comparative study of the properties of several oily additives of different chemical structure (one branched two-chain alkanol, one two-chain ester, two *n*-alkanols of different chain lengths, a long-chain saturated hydrocarbon, and silicone oil—see Figure 2) in SDDBS solutions. The major aims of the study are (1) to compare the effect of these oils on the foaminess and the foam stability of the surfactant solutions, (2) to analyze the obtained results from the viewpoint of the dynamic and static interfacial properties, and (3) to explore the importance of the so-called "entry barrier",[6−13,26−30] which is connected to the stability of the asymmetric oil−water−air films and to the possibility for emergence of the emulsified oil onto the foam film surface (Figure 1). The first paper in this series concerns primarily aims 1 and 2, while the second paper[31] describes and discusses

(14) Abe, Y.; Matsumura, S. *Tenside Deterg.* **1983**, *20*, 218.
(15) Ivanov, I. B. *Pure Appl. Chem.* **1980**, *52*, 1241.
(16) Ivanov, I. B.; Dimitrov, D. S. In *Thin Liquid Films*: *Fundamentals and Applications*; Surfactant Science Series; Ivanov, I. B., Ed.; Marcel Dekker: New York, 1988; Vol. 29, Chapter 7.
(17) Kralchevsky P. A.; Danov, K. D.; Ivanov, I. B.; Chapter 1 in ref 1.
(18) Danov, K. D.; Kralchevsky, P. A.; Ivanov, I. B. In *Handbook of Detergents*, *Part A*: *Properties*; Broze, G., Ed.; Surfactant Science Series; Marcel Dekker: New York, 1999; Chapter 9; Vol. 82.
(19) Narsimhan, G.; Ruckenstein, E. Chapter 2 in ref 1.
(20) Patist, A.; Axelberd, T.; Shah, D. O. *J. Colloid Interface Sci.* **1998**, *208*, 259.
(21) Brown, A. G.; Thuman, W. C.; McBain, J. W. *J. Colloid Sci.* **1953**, *8*, 491.
(22) Jones, M. N.; Reed, D. A. *J. Colloid Interface Sci.* **1969**, *30*, 577.
(23) Bergeron, V. Ph.D. Thesis, University of California, Berkeley, 1993.
(24) Lu, J. R.; Purcell, I. P.; Lee, E. M.; Simister, E. A.; Thomas, R. K.; Rennie, A. R.; Penfold, J. *J. Colloid Interface Sci.* **1995**, *174*, 441.
(25) Angarska, J. K.; Tachev, K. D.; Kralchevsky, P. A.; Mehreteab, A.; Broze, G. *J. Colloid Interface Sci.* **1998**, *200*, 31.
(26) Bergeron, V.; Fagan, M. E.; Radke, C. J. *Langmuir* **1993**, *9*, 1704.
(27) Lobo, L.; Wasan, D. T. *Langmuir* **1993**, *9*, 1668.
(28) Kulkarni, R. D.; Goddard, E. D.; Kanner, B. *J. Colloid Interface Sci.* **1977**, *59*, 468.
(29) Koczo, K.; Lobo, L. A.; Wasan, D. T. *J. Colloid Interface Sci.* **1992**, *150*, 492.
(30) Aveyard, R.; Binks, B. P.; Fletcher, P. D. I.; Peck, T.-G.; Garrett, P. R. *J. Chem. Soc., Faraday Trans.* **1993**, *89*, 4313.
(31) Hadjiiski, A.; Tcholakova, S.; Denkov, N. D.; Ivanov, I. B.; Durbut, P.; Broze, G.; Mehreteab, A. *Langmuir* **2001**, *17*, 7011−7021.

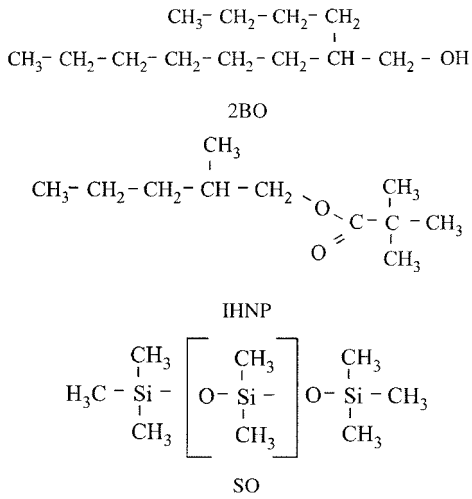

Figure 2. Structural formulas of some of the studied oils: 2-butyloctanol, 2BO; isohexyl neopentanoate, IHNP; silicone oil, SO. The other studied oils are *n*-heptanol, *n*-C_7OH; *n*-dodecanol, *n*-$C_{12}OH$; and *n*-hexadecane, *n*-C_{16}.

results about the entry barriers for the studied oils (aim 3), as obtained by the recently developed film trapping technique (FTT).[32,33]

2. Experimental Details

2.1. Materials and Preparation Procedures. Sodium dodecylbenzenesulfonate, SDDBS ($C_{12}H_{25}C_6H_4SO_3Na$, 99% purity, produced by Aldrich, Steinheim, Germany), is used as a main surfactant at a concentration of 0.09 wt %, which is 2.6 mM or approximately 13×cmc. The working solutions contain also 12 mM NaCl (p.a. Merck, heated at 500 °C before utilization) and 0.01 wt % (unless another value is specified) of the oily additive. As additives we studied 2-butyloctanol, 2BO (trade name Isofol 12, Condea Chemie GmbH, Hamburg, Germany), *n*-dodecanol, *n*-$C_{12}OH$ (Sigma Chemical Co., St. Louis, MO), *n*-heptanol, *n*-C_7OH (Sigma), isohexyl-neopentanoate, IHNP (trade name Schercemol 65, Scher Chemicals, USA), silicone oil SH200 of dynamic viscosity 5 mPa·s (Kao Co., Tokyo, Japan), SO, and *n*-hexadecane, *n*-C_{16} (Sigma). Hexadecane is refined by passing it through a glass column filled with chromatographic adsorbent Florisil.[34] The other chemicals are used as received. The solutions are prepared with deionized water from a Milli-Q Organex system (Millipore).

The oily additives are emulsified by two different procedures to study the effect of the oil drop size: (1) 0.05 g oil is introduced into 150 mL of the surfactant solution and an intensive stirring for 1 h on a magnetic stirrer is employed. The obtained emulsion is diluted to a volume of 500 mL to obtain the working concentration of 0.01 wt %; the emulsion is additionally homogenized by several hand-shakes before using it in the foam tests. (2) A 0.1 g portion of the oily additive is introduced into a 150 mL laboratory beaker containing 100 mL of surfactant solution and an agitation by a rotor-stator homogenizer Ultra Turrax T25 (Janke&Kunkel Gmbh&Co, IKA-Labortechnik, Germany) is applied for 20 s at 10 000 rpm. This emulsion is afterward diluted by surfactant solution to the desired oil concentration, and the obtained working solution is immediately used. For brevity, we call hereafter the emulsions produced by magnetic stirring the coarse emulsions, while those obtained by the rotor-stator homogenizer are termed the fine emulsions (the respective drop size distributions are discussed in section 3.4).

Most of the used additives are partially soluble in the surfactant solutions, mainly due to solubilization in the surfactant micelles. To separate the effects created by the oily drops from the effects due to molecularly solubilized oil, in some of the experiments we use pre-equilibrated surfactant solutions, from which the drops are removed as completely as possible. After 24 h of pre-equilibration with 0.01 wt % of additive under continuous stirring, the surfactant solution is kept at rest for 48 h in a separation funnel for a gravity-driven separation of the oil drops. The lower portion of the solution is drained from the funnel and centrifuged at 5000*g* for at least 3 h. The upper layer of the liquid is removed from the centrifugal vial by suction, and finally, the remaining solution is filtered twice through a 220 nm membrane filter. Even this complex procedure does not result in a complete removal of the oil drops as evidenced by the scattering of light when a laser beam is propagating through the precleaned solution. However, the oil concentration in these solutions is much lower as compared to that in the working solutions containing 0.01 wt % of oil.

2.2. Methods. 2.2.1. Foam Formation and Foam Stability Evaluation. The Ross-Miles test is used in most of the experiments to produce foams and to compare their stability. A glass cylinder of 520 cm^3 volume and 37 mm diameter is connected to a pump, which drives the circulation of the surfactant solution (300 mL). The liquid is pumped for 20 s, at a rate of 125 cm^3/s through an orifice, 7 mm in diameter, which is placed at 23 cm above the level of the liquid. The change of the foam volume with time is monitored for a period of 15 min after liquid circulation ceases. From the diameter of the cylinder of the Ross-Miles test, one can calculate that a reduction of the foam volume by 10 mL corresponds to a decrease of the foam height by ≈1 cm. The accuracy in the foam volume determination is ±5 mL, whereas the reproducibility is typically ±10 mL.

In another set of experiments, the foam is produced by five rigorous hand shakes of 100 mL glass cylinders containing 20 mL of surfactant solution. Afterward, a 10 μL oil drop is placed on the wall of the cylinder (5 cm above the top of the foam column) and the foam destruction by the spreading oil is monitored for 10 min.

2.2.2. Size Distribution of Emulsion Droplets. The size distribution of the emulsion droplets is determined by video-microscopy observations (microscope Studar M, PZO, Warsaw, Poland; objectives 50× and 100×) in white transmitted light. The image is recorded by a high-resolution CCD camera (Sony SSC-M370 CE) and digital memory VCR (Panasonic AG-7355). The recorded images are processed by homemade image analysis software for determining the drop size distribution. The diameter of several hundreds drops is typically measured in each sample. The optical resolution of the used system is approximately 1 μm.

2.2.3. Surface and Interfacial Tension Measurements. Ellipsometry. The surface tension of the surfactant solution is measured by the Wilhelmy plate method on a Kruss K10T digital tensiometer. After the surface tension of the solution is measured in the absence of oil, an oil drop of 15−30 μL is gently deposited by a pipet on the solution surface away from the Wilhelmy plate. The reduction of the surface tension, due to spreading of the oil over the surface, is monitored afterward. The thickness of the spread oil layer is measured ellipsometrically by using the equipment from ref 35 and the procedure described in ref 36. These experiments are performed in closed containers to reduce the evaporation of oil and water from the solution surface.

The surface tension of bulk oils is measured by the Du Nouy ring technique on a Kruss K10T tensiometer. To check whether the surfactant solution spreads over the oil surface, we first measure the surface tension of pure oil. Then a drop of the surfactant solution is carefully placed in contact with the oil surface for at least 1 min, and the surface tension of the oil is measured again (no change of the oil surface tension was detected for all of the studied systems). The tension of the oil−solution interface is measured by a homemade pendant drop method or the spinning drop method (Kruss Site 04 tensiometer).

The entry, *E*, spreading, *S*, and bridging, *B*, coefficients are calculated from the interfacial tensions

(32) Hadjiiski, A.; Dimova, R.; Denkov, N. D.; Ivanov, I. B.; Borwankar, R. *Langmuir* **1996**, *12*, 6665.
(33) Hadjiiski, A.; Tcholakova, S.; Denkov, N. D., Ivanov, I. B. *Proceedings of the 13th Symposium on Surfactants in Solution* (*SIS 2000*); Gainsville, FL, June 2000, in press. Hadjiiski, A.; Tcholakova, S.; Ivanov, I. B.; Gurkov, T. D.; Leonard, E. *Langmuir*, in press.
(34) Gaonkar, A. *J. Am. Oil Chem. Soc.* **1989**, *66*, 1090.
(35) Russev, S. C.; Argirov, T. V. *Rev. Sci. Instrum.* **1999**, *70*, 3077.
(36) Denkov, N. D.; Marinova, K. G.; Christova, C.; Hadjiiski, A.; Cooper P. *Langmuir* **2000**, *16*, 2515.

$$E = \sigma_{AW} + \sigma_{OW} - \sigma_{OA} \quad (1)$$

$$S = \sigma_{AW} - \sigma_{OW} - \sigma_{OA} \quad (2)$$

$$B = \sigma_{AW}^2 + \sigma_{OW}^2 - \sigma_{OA}^2 \quad (3)$$

The subscripts AW, OW, and OA refer to air−water, oil−water, and oil−air interfaces, respectively; σ_{AW} denotes either the surface tension in the absence of oil (so-called initial E_{IN}, S_{IN}, and B_{IN} coefficients) or the tension after spreading of oil on the solution surface (equilibrium E_{EQ}, S_{EQ}, and B_{EQ}). The positive initial spreading coefficient, S_{IN}, indicates either a spreading of oil on the solution surface as a multimolecular layer or a formation of mixed adsorption layer of surfactant and oil molecules.[30] The equilibrium spreading coefficient, S_{EQ}, could be either negative (oil lenses are formed on the solution surface) or zero (complete spreading of the oil as a duplex film).[37] The role of these coefficients in the antifoaming action of oils is discussed in refs 7−12. In general, positive values of E and B are considered to be a necessary (but insufficient) condition for having an active oil. Recent studies[7,38] show that positive values of S are not a necessary condition for having an antifoaming activity of the oil, though the spreading might be helpful in some cases.[10,31,39]

The dynamic surface tension of the solutions is measured by the maximum bubble pressure method (MBPM) on homemade equipment, which is described in ref 40. A hydrophobic capillary with a hydrophilic tip and the standard procedure for calculation of the surface tension from the maximum pressure are used (without a video-recording and image analysis of the bubble shape).

2.2.4. Stability of Foam Films. Horizontal foam films of diameter ≈1 mm are formed and observed in a Scheludko cell.[41,42] A foam film is formed from a biconcave drop of surfactant solution, placed in a vertical cylindrical glass capillary, by sucking out liquid through an orifice in the capillary wall. The film radius can be varied by a pressure control system. Special care is taken to suppress the water evaporation. The films are observed from above (microscope Zeiss Axioplan, objectives LD Epiplan 10× and 50×) in reflected or transmitted white light. The observations in reflected light provide a clear picture of the foam films, while the transmitted light allows one to observe oil drops in the film or in the adjacent meniscus region.[6]

In another set of experiments, the porous plate method of Mysels[2,23,43,44] is used to evaluate the critical capillary pressure inducing a rupture of the foam film. The liquid in the experimental cell is in contact with a pressure transducer (Omega PC136G1), which measures the pressure difference between the liquid phase and the ambient atmosphere (i.e., the capillary pressure). A correction for the hydrostatic pressure difference between the plane of the foam film and the level of the transducer membrane is employed. The maximum capillary pressure attainable by the porous plate method is 5000 Pa, while the typical capillary pressure in the Scheludko cell is about 40 Pa.

2.2.5. Measurement of the Elasticity of Water−Air Interface by the Expanding Drop Method (EDM). A homemade equipment is used to determine the dilatational surface elasticity, E_{SD}, of the surfactant solution around the cmc (0.35 mM SDDBS, 12 mM NaCl solution). The equipment consists of a glass capillary, which is connected to a piezoresistive pressure transducer (163PC01D36, Omega) and two microsyringes (no. 1 of 100 μL and no. 2 of 1 mL); see Figure 3. Syringe 1 is driven by a dc motor (Newport 860A) and provides a constant liquid flow. The two syringes, the working orifice of the pressure transducer, and the capillary are filled with surfactant solution. The electrical signal from the pressure transducer is amplified and recorded on a computer via an analog-to-digital converter (ADC). A drop of the surfactant solution is formed on the tip of the capillary and is observed by an optical microscope. The whole system is mounted in a closed container, whose bottom is covered by the investigated solution, to suppress the evaporation of water and oil.

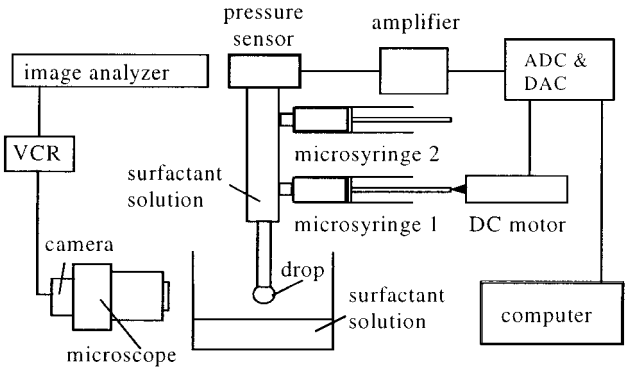

Figure 3. Experimental setup for determination of surface dilatational elasticity, E_{SD}, by the expanding drop method, EDM.

The experiment is carried out as follows. The experimental setup is filled with surfactant solution, and a drop is formed on the capillary tip by using syringe 2. The drop volume is kept constant for 1−4 h (depending on the particular system) to achieve an equilibrium adsorption of surfactant on the drop surface. From the capillary pressure, P_C, and the drop radius, R, measured by the pressure transducer and by the microscope, respectively, one can calculate the equilibrium surface tension of the solution, $\sigma_{AW}^{EQ} = (P_C R)/2$. Afterward, a controlled expansion of the drop surface is accomplished for 1−25 s by squeezing a solution out of the capillary (syringe 1 is used at this stage). The changes of the total stress $\tau(t) = [P_C(t)R(t) - P_C(0)R(0)]/2$, and of the drop area, $A(t)$, are monitored during the expansion.

The experimental data are processed by using a simple rheological model

$$\tau = E_{SD}\,\alpha \quad (4)$$

where E_{SD} is the surface dilatational elasticity and $\alpha = \ln(A/A_0)$ is the relative change of the surface area. This model implies that one can calculate the surface elasticity from the initial slope of the experimental curve (where τ is a linear function of α), neglecting the effects of surfactant adsorption and viscous dissipation in the beginning of the drop expansion process. In the absence of viscous stresses, τ has the meaning of a deviation of the surface tension during expansion from its equilibrium value, $\tau = \sigma_{AW}(t) - \sigma_{AW}^{EQ}$. Therefore, the obtained value of E_{SD} corresponds to an effective surface elasticity, which does not necessarily coincide with the thermodynamically defined Gibbs elasticity, E_G. The experiments are performed around the cmc of SDDBS, because the surface stress created in the experiments with the working solutions (2.6 mM) is too small to be reliably detected and interpreted.

To study the effect of the spread layer of IHNP on the surface elasticity of the surfactant solution, some of the experiments are performed with drops whose surfaces are covered by a spread layer of IHNP. Such drops are formed in the following way: First, the experimental setup is filled with surfactant solution and an aqueous drop is formed from the solution on the tip of the capillary, as described above. Next, IHNP is spread on the surface of the bulk solution, which is placed in the container below the capillary; see Figure 3. The capillary is moved downward until the drop coalesces with the bulk solution (i.e., an aqueous bridge is formed between the capillary and the bulk solution). Finally, the capillary is detached from the surface of the bulk solution by moving it upward. Thus a drop of the surfactant solution is formed again, with a spread layer of IHNP being transferred from the surface of the bulk solution onto the drop surface. After several hours

(37) Rowlinson, J. S., Widom, B. *Molecular Theory of Capillarity*; Oxford University Press: Oxford, 1989; Chapter 8.
(38) Garrett, P. R.; Davis, J.; Rendall, H. M. *Colloids Surf., A* **1994**, *85*, 159.
(39) Denkov, N. D.; Marinova, K. *Proceedings of the 3rd EuroConference on Foams, Emulsions and Applications*; MIT: Bremen, 2000; p 199.
(40) Horozov, T. S.; Dushkin, C. D.; Velev, O. D.; Danov, K. D.; Arnaudov, L. N.; Mehreteab, A.; Broze, G. *J. Colloid Interface Sci.* **1996**, *113*, 117.
(41) Scheludko, A.; Exerowa, D. *Kolloid Z.* **1957**, *155*, 39.
(42) Scheludko, A. *Adv. Colloid Interface Sci.* **1967**, *1*, 391.
(43) Mysels, K.; Jones, A. *J. Phys. Chem.* **1964**, *68*, 3441.
(44) Claesson, P. M.; Ederth, T.; Bergeron, V., Ruthland, M. W. *Adv. Colloid Interface Sci.* **1996**, *67*, 119.

Table 1. Measured Interfacial Tensions and Calculated Entry, *E*, Spreading, *S*, and Bridging, *B*, Coefficients for Different Oils[a]

additive	σ_{AW}^{EQ}, mN/m	σ_{OW}, mN/m	σ_{OA}, mN/m	E_{IN}, mN/m	E_{EQ}, mN/m	S_{IN}, mN/m	S_{EQ}, mN/m	B_{IN}, (mN/m)^2	B_{EQ}, (mN/m)^2	P_C^{CR}, Pa
2BO	27.7	3.6	26.5	7.7	4.8	0.5	−2.4	247	78	44
IHNP	24.8	1.8	23.6	8.8	3.0	5.2	−0.6	383	61	73
n-C_{12}OH	24.5	6.0	27.8		2.7		−9.3		−137	>1500
n-C_7OH	27.9	4.6	25.6		6.9		−2.3		144	*b*
SO	23.5	5.6	18.7	17.5	10.4	6.3	−0.8	618	234	>3000
n-C16	30.0	2.8	27.2	6.2	5.6	0.6	0.0	204	168	≈400

[a] σ_{AW}^{IN} is 30.6 mN/m in all cases except for *n*-C_{12}OH, where it is 30.2 mN/m (at 27 °C). The accuracy of the calculated values of *E* and *S* is ±1 mN/m; for *B* it is ±15 mN/m. [b] Not measured.

at rest (for reaching the equilibrium surface tension), this drop is expanded as described above.

All experiments are performed at an ambient temperature of 25 ± 2 °C, except those with *n*-C_{12}OH, which are performed at 27 ± 0.2 °C to avoid the oil crystallization (the melting point of *n*-C_{12}OH is around 24 °C).

3. Results and Discussion

First, results from model experiments with different oils are presented. Next, the foaminess and the foam stability of the surfactant solutions are discussed and explained on the basis of the results from the model experiments.

3.1. Entry (*E*), Spreading (*S*), and Bridging (*B*) Coefficients, Entry Barriers. 3.1.1. Oil Spreading. The measured interfacial tensions and the calculated values of *E*, *S*, and *B* coefficients are presented in Table 1. The initial coefficients for *n*-C_{12}OH and *n*-C_7OH are not presented, because these two alkanols are more soluble in the SDDBS solutions than the other studied oils. As a result, an intensive mass transfer across the oil−water interface is observed by optical microscopy when a drop of *n*-C_{12}OH or *n*-C_7OH is placed in contact with the solution. Therefore, the interfacial tensions, σ_{OW}, which can be measured only with pre-equilibrated phases, cannot be used to calculate the initial *E*, *S*, and *B* coefficients for these two alkanols. Direct measurements showed that the surface tension of the SDDBS solutions decreases very rapidly by several mN/m when a drop of *n*-C_{12}OH or *n*-C_7OH is placed on the solution surface. This observation proves that both alkanols rapidly spread, i.e., that S_{IN} is positive. There is no problem to determine the equilibrium coefficients for all oils, because the interfacial tensions are measured with pre-equilibrated phases.

The results show that the initial spreading coefficients of the remaining oils are all positive. It is worth noting that the oils possessing a relatively large $S_{IN} > 5$ mN/m (IHNP and SO) spread very rapidly—the surface tension reduction after placing the oil drop on the solution surface occurs for less than 1 s. On the contrary, 2BO and *n*-C_{16}, which possess $S_{IN} \approx 0.5$ mN/m (actually, this value is smaller than the accuracy of our determination, ±1 mN/m) exhibit much slower kinetics of surface tension reduction, on the order of several minutes.

The observed qualitatively different spreading kinetics of the studied oils is probably related to different structure of the formed spread layers. As discussed by Binks et al.,[45] some oils are only involved in a "chain mixing"—a process that leads to formation of a mixed adsorption layer with the surfactant molecules, without an actual spreading of a continuous oil layer on the solution surface. The main driving force for this process is the gradient of the surface concentration of oil molecules in the mixed adsorption layer, which suggests that the surface diffusion (which is a relatively slow process) leads to establishment of the equilibrium surface tension in these systems. Other oils, however, spread as continuous layers—thick or thin, depending on the disjoining pressure acting across the oil film.[45] The main driving force for such spreading is the initial spreading coefficient, S_{IN}, which represents the difference in the interfacial tensions acting on the three-phase contact line. As shown by Bergeron et al.[46,47] with several surfactants above their cmc, the oil spreading in this case is very fast and obeys a simple hydrodynamic law.

Indeed, visual observations and measurements by ellipsometry show that IHNP spreads rapidly and completely as a thick oil layer (so-called duplex film[7]) on the surface of SDDBS solutions. This spreading behavior is in agreement with the measured equilibrium spreading coefficient for IHNP, which is virtually zero in the framework of the experimental accuracy. In contrast, when 2BO is placed on the solution surface, several oil lenses are formed and the surface tension slowly decreases (by about 2 mN/m for 20 min) but no spread layer is detected by ellipsometry. Even after 1 h, the ellipsometrical signal remains unchanged, which means that the thickness of the adsorption layer is not affected by the spreading oil (the resolution of the equipment is about 0.1 nm). These results show that a monomolecular, mixed adsorption layer of SDDBS and 2BO is formed on the solution surface, in coexistence with lenses of 2BO.

One may speculate that the faster oil spreading should lead to a more efficient foam destruction—the results from our foam stability tests, however, do not support such a general trend (section 3.6), which means that other factors are more important.

3.1.2. Entry and Bridging Coefficients, Entry Barriers. As seen from Table 1, the values of all entry and bridging coefficients are positive except the negative equilibrium bridging coefficient determined with *n*-C_{12}OH. The positive bridging coefficients indicate that the oil bridges would be unstable if they are formed in the foam films.[7,10] On the other side, the formation of oil bridges from pre-emulsified oil drops requires the rupture of the asymmetric oil−water−air films, formed between the drops and the solution surface (Figure 1). As seen from Table 1, the studied oils exhibit rather diverse entry barriers: for 2BO and IHNP the barrier is below 100 Pa, for *n*-C_{16} it is 400 Pa, while for *n*-C_{12}OH and SO it is much higher (above 1500 and 3000 Pa, respectively). The entry barrier for *n*-C_7OH could not be measured by the FTT for technical reasons, which are described in ref 31. However, the results obtained by Kruglyakov,[11−13] and the poor foam stability in the presence of *n*-C_7OH drops, suggest that the entry barrier for this oil is low.

(45) Binks, B. P.; Crichton, D.; Fletcher, P. D. I.; MacNab, J. R.; Li, Z. X.; Thomas, R. K.; Penfold, J. *Colloids Surf., A* **1999**, *146*, 299.

(46) Bergeron, V.; Cooper, P.; Fischer, C.; Giermanska-Kahn, J.; Langevin, D.; Pouchelon, A. *Colloids Surf., A* **1997**, *122*, 103.

(47) Bergeron, V.; Langevin, D. *Phys. Rev. Lett.* **1996**, *76*, 3152.

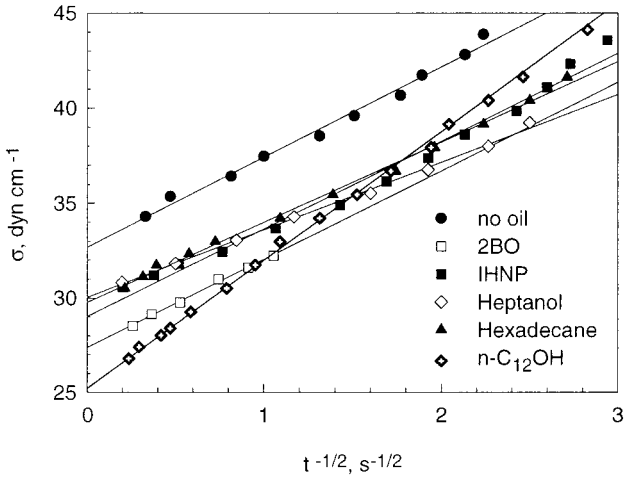

Figure 4. Dynamic surface tension (DST) of solution containing 2.6 mM SDDBS, 12 mM NaCl, and 0.01 wt % of different oils (coarse emulsion) as a function of $t^{-1/2}$.

As discussed below, the entry barrier is among the most important factors determining the activity of a given oil as a foam breaker.

3.2. Dynamic Surface Tension (DST). In principle, the DST of micellar surfactant solutions can be affected by oils via two different mechanisms. The first one is related to the molecular diffusion and adsorption of surfactant and oil molecules on the solution surface. The rate of surfactant adsorption in micellar solutions is influenced by the demicellization rate.[20,48−50] The presence of solubilized oil in the micelles could strongly affect the demicellization rate and the kinetics of surfactant adsorption. In addition, part of the solubilized oil molecules could also adsorb on the solution surface after their release from the micelles—these oil molecules would participate in the formation of mixed adsorption layer, reducing in this way the DST. The second mechanism of surface tension reduction, in the presence of oil, consists of coalescence of dispersed oil drops with the solution surface (drop entry), followed by oil spreading. Therefore, the barrier to drop entry, the rate of oil spreading, and S_{IN} (which determines the magnitude of the surface tension reduction by the spread oil) are other important factors for the DST of such systems.

The DST of the working solutions, measured by the MBPM, is shown in Figure 4. Experiments with SDDBS solutions in the absence and in the presence of 0.01 wt % of oil (coarse emulsion) are performed. No experiments with SO were made to avoid contamination of the experimental equipment with this difficult-for-cleaning oil. Remarkably, the curves for most of the oils lay very close to each other in the range of bubble lifetimes from 0.2 to 4 s. One can notice that all of the oils reduce the DST by 4−6 mN/m in the interval between 0.5 and 2 s. This similarity in the DST curves is surprising (and probably fortuitous) having in mind the diverse chemical structure of the studied oils, which determines a rather different spreading behavior and, probably, different rates of demicellization in the studied solutions.

The only curve that deviates significantly from the others is that of *n*-C_{12}OH. This curve has a notably larger slope, which is caused by (i) the high surface activity of *n*-C_{12}OH, which leads to lower equilibrium surface tension as compared to the other oils, see Table 1, and (ii) a relatively low rate of demicellization in the presence of *n*-C_{12}OH, which decelerates the surfactant adsorption at short times. Indeed, Patist et al.[20] found that the addition of *n*-C_{12}OH to SDS solutions leads to reduced rates of demicelization and surfactant adsorption—a similar effect can be expected in SDDBS solutions as well.

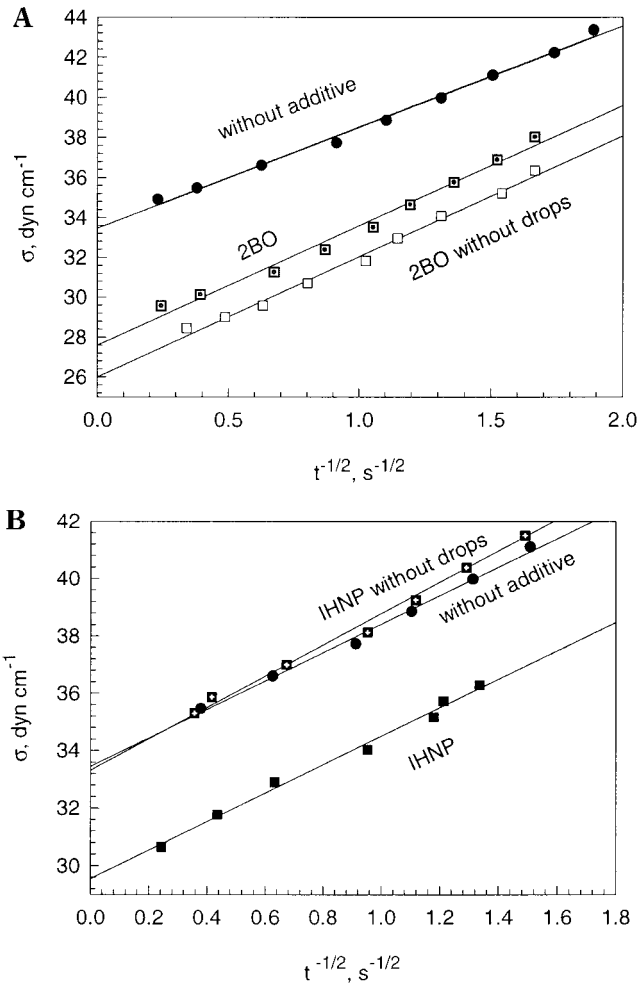

Figure 5. Dynamic surface tension of solutions containing 2.6 mM SDDBS and 12 mM NaCl in the absence of oil, in the presence of 0.01 wt % oil (coarse emulsion), and after the oil drops have been removed: (A) 2BO, (B) IHNP solutions (see sections 2.1 and 3.2).

To separate the effect of the oil drops on the DST, we made experiments with solutions that were pre-equilibrated with 2BO and IHNP, and the oil drops were afterward removed as explained in section 2.1. The results (see Figure 5) show that the drop-deprived solutions of 2BO show virtually the same DST as those of the working solutions containing drops. Therefore, 2BO reduces the DST mainly by the molecular mechanisms mentioned above, namely, by increasing the rate of demicellization and by molecular diffusion and adsorption of oil molecules onto the surface. On the contrary, solutions deprived of IHNP drops show virtually the same DST as that of the pure surfactant solution. Hence the surface tension reduction in the IHNP-containing solutions occurs primarily through a coalescence of oil drops with the solution surface.

The importance of these results for the foamability of the surfactant solutions is discussed in section 3.6 below.

(48) Joos, P. *Dynamic Surface Phenomena*; VSP: Zeist, The Netherlands, 1999.

(49) Dukhin, S. S.; Kretzschmar, G.; Miller, R. *Dynamics of Adsorption at Liquid Interfaces*; Elsevier: Amsterdam, 1995.

(50) Dushkin, C. D.; Ivanov, I. B.; Kralchevsky, P. A. *Colloids Surf.* **1991**, *60*, 235.

Table 2. Surface Dilatational Elasticity, E_{SD}, of 0.35 mM SDDBS Solution in the Presence of 12 mM NaCl with Coarse Emulsion and with a Spread Layer of Additive (see the text for details)[a]

	E_{SD}, mN/m	
additive	emulsion	spread layer
IHNP	18 ± 5	1.5 ± 0.5
2BO	12 ± 4	12 ± 5
n-C_{12}OH	24 ± 4	

[a] E_{SD} = 13 ± 1 mN/m in the absence of oil.

3.3. Dilatational Elasticity of the Water−Air Interface. The surface elasticity of the foaming solution is another characteristic related to its foamability. Higher elasticity corresponds to a more rapid increase of the surface tension during surface expansion, which would require more energy to create new bubbles during foam generation at equivalent other conditions.

The surface elasticity of 0.35 mM SDDBS solutions in the absence of oil additives was determined by EDM to be E_{SD} = 13 ± 1 mN/m. The results obtained with 0.01 wt % coarse emulsions of IHNP and 2BO were very similar to those in the absence of oil (see Table 2). In the case of *n*-C_{12}OH emulsion, however, the obtained surface elasticity was about twice higher, E_{SD} = 24 ± 4 mN/m, which is due to formation of a particularly dense mixed adsorption layer from the main surfactant and the alcohol.[24] The large value of E_{SD} agrees qualitatively with the measured steeper dependence of the DST on the bubble lifetime (Figure 4), as well as with the relatively low foamability of the solutions containing C_{12}OH (Figure 9 below). On the other side, as discussed in the literature,[15−18] the higher surface elasticity decelerates the thinning of the foam films and stabilizes them against rupture.

Since the results described in section 3.2 show that the reduction of DST of SDDBS solutions by IHNP is due to coalescence of oil drops with the solution surface, we performed EDM experiments with surfactant solutions whose surface was covered by a spread layer of IHNP. The presence of a spread IHNP drastically changes the observed rheological behavior of the solution surface. In Figure 6A the total strain, α, for two different experiments, with emulsion of IHNP and with a spread layer of the same oil, is plotted as a function of time. One sees that the magnitude and the rate of surface expansion in these two experiments are very similar, while the measured surface stresses are very different, Figure 6B. The slope of the surface stress in the case of spread IHNP layer is an order of magnitude smaller (E_{SD} = 1.5 ± 0.5 mN/m) than the one in the experiments with IHNP emulsion and in the absence of oil (13−18 mN/m).

In principle, one could try to explain this low value of E_{SD} by assuming that a thick uniform layer of IHNP is present on the surface of the aqueous drop throughout its expansion. If this were the case, then the measured elasticity should be equal to the elasticity of the oil−water interface, which is formed between the spread layer and the aqueous drop (or larger if the oil−air interface also contributes to the measured surface elasticity). However, direct measurements of the oil−water interfacial elasticity with aqueous drops immersed in bulk IHNP showed that it is too high, 5 ± 1 mN/m, to support the above explanation. That is why we suggest another interpretation of the low surface elasticity in the presence of a spread IHNP layer. We assume that the spread IHNP layer ruptures almost immediately after the drop expansion has started—one or several oil lenses are formed on the drop surface (Figure 7), which serve as a reservoir of oil throughout the period of surface expansion. Since the spreading of the precursor oil film is a very fast process,[46,47] the surface of the expanding drop would be always covered with a thin oil layer, which decreases the surface tension and the measured surface stress. With respect to foaming, this corresponds to lower dynamic surface tension in the presence of spread oil, which might explain the enhanced foamability of IHNP-containing solutions in a certain range of oil concentrations (see section 3.6.4 and Figure 10A below), where presumably the coalescence of oil drops with the bubbles results in the formation of a spread IHNP layer.

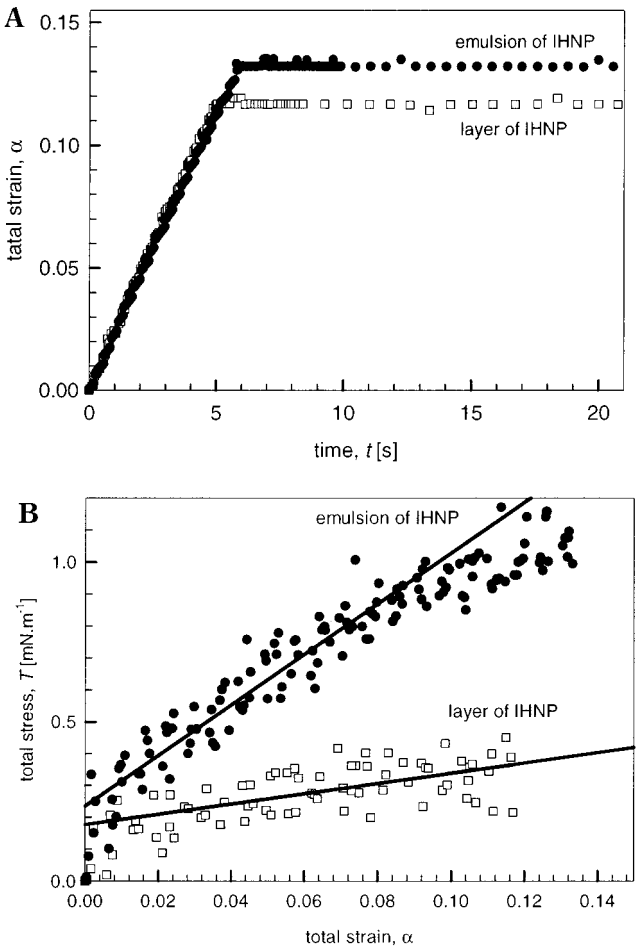

Figure 6. Experimental data obtained by EDM: (A) surface strain, α, vs time for emulsion of IHNP (circles) and for a spread layer of IHNP (boxes); (B) stress τ vs α for the same experiments. The surface dilatational elasticity is calculated from the slope of the lines drawn in (B). All solutions contain 0.35 mM SDDBS and 12 mM NaCl.

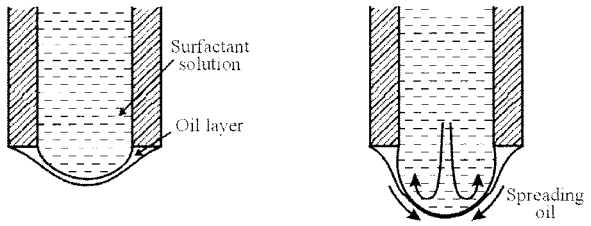

Figure 7. A possible explanation of the measured low surface elasticity of an aqueous drop in the presence of a spread IHNP layer. The expansion of the drop surface leads to rupture of the oil layer—the subsequent surface expansion is accompanied with a fast spreading of oil from the thicker oil regions (acting as reservoirs), so that the drop surface is always covered with a thin oil layer, which maintains low surface stress.

One can notice in Figure 6B that there is some positive intercept of the dependence $\tau(\alpha)$. This intercept is due to several phenomena accompanying the start of the drop expansion process, such as the effect of liquid viscosity (hydraulic shock), the initial nonlinear motion of the dc motor, some mechanical disturbances, etc., that is, this intercept is an artifact created by the used equipment.

3.4. Oil Solubility in the Surfactant Solution and Drop Size Distribution. Microscope observations and light-scattering experiments showed that all of the studied oils (except *n*-C_7OH) were not completely dissolved in the surfactant solutions at the working concentration of 0.01 wt %—a fraction of the oil remained in the form of dispersed drops. The solubility of *n*-C_7OH was determined by measuring the intensity of light scattered from SDDBS solutions, in which different volumes of *n*-C_7OH were added. These measurements were made 5 days after the introduction of *n*-C_7OH in the solutions. A sharp increase of the intensity of the scattered light was observed at *n*-C_7OH concentrations around 0.15 wt %, which means that its solubility is about 0.15 ± 0.05 wt %. We were unable to determine the solubility of the other oils, because it was very low (below 0.005 wt %).

The drop size distribution in the samples containing 2BO and IHNP was determined to check the reproducibility of the emulsification procedure and to compare the drop size with the cross section of the Plateau borders (GPBs). Measurements of four independently prepared samples of fine 2BO emulsion (0.1 wt %, emulsified by Ultra Turrax, see section 2.1) showed approximately log-normal distribution with a geometrical mean drop radius of 1.9 μm and polydispersity $\sigma_g = 2.0$; 200 drops were measured in each sample. Most of the drops fell in the range between 0.8 and 5 μm, but larger drops of radius up to 10 μm were occasionally observed in the samples. Virtually the same drop size distribution was determined in samples prepared at the working oil concentration of 0.01 wt %; 100 drops were counted in this experiment. A very similar drop size distribution (mean radius 1.8 μm; $\sigma_g = 2.2$) was determined also in four independently prepared samples containing fine emulsions of IHNP.

The oil drops in the coarse emulsions (prepared on magnetic stirrer) were somewhat larger—the mean drop radii were 2.2 μm in 2BO and 2.9 μm in IHNP emulsions and drops of radius as large as 20 μm were occasionally observed in these samples. The reproducibility of the size distribution in the coarse emulsions was lower as compared to the one in the fine emulsions.

As discussed in section 3.5 below, the studied oils destroy foam by rupturing the Gibbs−Plateau borders (not foam films). To compare the size of the oil drops with the cross section of the Gibbs−Plateau borders (Figure 1), one should estimate the radius of curvature, R_{PB}, of the GPB wall. As explained in ref 6, R_{PB} in the top layer of a foam column of height H can be estimated from the conditions for hydrostatic equilibrium

$$R_{PB}(H) = \sigma_{AW}/P_C \approx \sigma_{AW}/(\Delta\rho g H) \qquad (5)$$

where $P_C(H)$ is the capillary pressure bubble−Plateau border, which is approximately equal to the hydrostatic pressure, $\Delta\rho g H$; $\Delta\rho$ is the difference between the mass densities of the aqueous and gaseous phases and g is the acceleration of gravity. Equation 5 predicts that $R_{PB} \approx 30$ μm at equilibrium for a foam column of height $H = 10$ cm, and $R_{PB} \approx 300$ μm for $H = 1$ cm. A geometrical consideration shows that the radius, R_D, of a sphere inscribed in the GPB (i.e., the minimal radius of a trapped sphere) is given by the expression

$$R_D(H) = R_{PB}(H)\left[\frac{3^{1/2}}{3}\sin\left(\frac{\pi}{6} - \theta_F\right) + \cos\left(\frac{\pi}{6} - \theta_F\right) - 1\right] \approx R_{PB}(H)\left[\frac{2(3^{1/2})}{3} - 1 - \frac{3^{1/2}}{3}\theta_F^2 + O(\theta_F^3)\right] \approx R_{PB}[0.155 - 0.577\theta_F^2] \qquad (6)$$

where θ_F (expressed in radians) is the half of the contact angle film−meniscus (Figure 1). Since the foam film thickness, $h \sim 10$ nm, is much smaller than R_{PB}, the film is considered infinitely thin in the derivation of eq 6. In most cases, $\theta_F < \pi/30$, which means that its contribution can be neglected; i.e., a reasonable estimate of R_D is given by the expression[6]

$$R_D(H) \approx 0.155\,\frac{\sigma_{AW}}{\Delta\rho g}\,\frac{1}{H} \qquad (7)$$

For a foam column with height $H = 10$ cm, eq 7 predicts $R_D \approx 5$ μm. This value is more than two times larger than the mean drop radius in our samples, which means that most of the oil drops are too small to cause foam destruction (unless many oil drops are closely packed in a single Plateau border). However, as explained above, oil drops of radius above 5 μm, which can be compressed by the narrowing walls of the GPB, are also present in the solutions. Moreover, a coalescence of the emulsion drops might occur in the GPBs during the liquid drainage, which would lead to an increase of the size of the drops captured in the foam.

One can conclude that the foam destruction in our systems is accomplished by the biggest drops, i.e., not only the mean size but also the polydispersity of the drops is important.

3.5. Foam films. 3.5.1. Foam Films in the Scheludko Cell. The experiments with small horizontal foam films in the Scheludko cell showed that the addition 0.01 wt % of the studied oils did not change significantly either the film-thinning rate or the equilibrium film thickness. No multiple stepwise transitions in the foam film thickness (stratification) were observed, because the concentration of micelles was too low. The final film thickness was 18 ± 1 nm, which corresponded to a common black film stabilized by electrostatic repulsion between the film surfaces (and possibly containing one layer of micelles, which does not leave the film spontaneously under these conditions). The oil drops left the foam films during their thinning without causing a film rupture, similar to the processes described in ref 6. Therefore, one can conclude that the drops are unable to rupture the thinning foam films, because the entry barriers are too high for drop entry to occur at this stage.[6,39]

3.5.2. Foam Films in the Mysels Cell. The porous plate method allows one to increase the suction capillary pressure exerted on the foam film and to determine the critical value, which induces a foam film rupture.[23,26,44] Since the presence of spread oil on the film surfaces could, in principle, lead to reduced stability of the foam films, we studied surfactant solutions, which were pre-equilibrated with IHNP and 2BO, and the oil drops were afterward removed (section 2.1). The experiments revealed that the foam films from these solutions are extremely stable and the critical capillary pressure for their rupture is above 5000 Pa. For comparison, the critical capillary pressure for entry of the oil drops is about 2 orders of magnitude lower; see Table 1. Therefore, one can conclude that the foam destruction in the presence of 2BO and IHNP is due to dispersed oil droplets (which are the actual

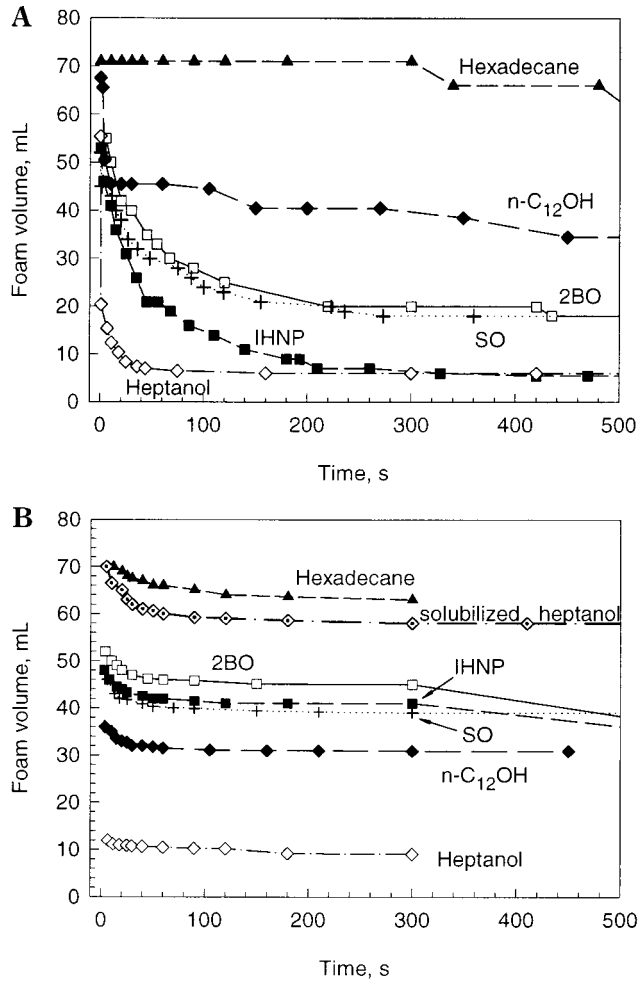

Figure 8. (A) Foam destruction by spreading of different oils on the top of a foam column formed from solution of 2.6 mM SDDBS and 12 mM NaCl. The oil emulsions (0.05 wt %) obtained after the end of experiment (A) are shaken again to produce foams, whose evolution is shown in (B). Another shaking cycle was made with these emulsions a week later, and the results were virtually the same as those presented in (B), except for heptanol which did not show any antifoam activity (see the respective curve in B), because it was already solubilized within the surfactant micelles.

antifoam entities) and is not related to reduced stability of the foam films. Similar conclusion for other systems (foams in porous media in the presence of hydrocarbons) was drawn previously by Bergeron et al.[26]

3.6. Foamability and Foam Stability. 3.6.1. Defoaming by Spreading of Oil over the Foam Column. The initial foam, $V_{IN} = 79$ mL, in these experiments is generated by five hand shakes of 20 mL of surfactant solution in the absence of oil. After 10 min at rest, the foam volume decreases to about 72 mL due to liquid drainage. At that moment, 10 μL of the oily additive is introduced on the top of the foam column, as described in section 2.2.1, and the foam decay is monitored for 10 min, Figure 8A. The strongest destabilizing effect is observed with *n*-C_7OH; the foam disappears almost completely within 20 s. Though more slowly (for 2−3 min), IHNP also leads to an almost complete foam destruction; the final foam volume of 6 mL is the same as with *n*-C_7OH. The deposition of 2BO and SO on the top of the foam column leads to similar decay profiles; after 2−3 min the foam volume levels off at about 20 mL. *n*-C_{12}OH leads to a moderate destruction of the foam down to about 35 mL. Only *n*-hexadecane is practically inactive as a defoamer at these conditions—a very slight reduction (by 4−5 mL) of the foam volume is detected during the observation period.

The solutions obtained after the above experiment were shaken again to check how the emulsified oils affect the foamability and the foam stability, Figure 8B. The initial foam volumes in the presence of oil were smaller than V_{IN} in the absence of oil. Most active as an antifoam is *n*-C_7OH ($V_{IN} = 12$ mL), while *n*-C_{16} has almost no effect ($V_{IN} = 70$ mL). The remaining additives result in intermediate V_{IN} between 35 and 50 mL. Note that these solutions contain 0.05 vol % oil, which means that the foam generation is strongly affected by the dispersed oil drops in the foaming medium (cf. with Figure 10 below). For about 5 min, the produced foams are stable in all systems. Afterward, a slow foam decay is observed in the presence of 2BO and IHNP (not shown in Figure 8B) and the foam volume in these systems reduces to 10−15 mL after 1 h, while the other foams remain stable during this period.

The differences in the defoaming activity of the oils added on the top of the foam column and the antifoam activity of the same oils when dispersed as drops in the foaming medium, cf. Figure 8, are due primarily to the decisive role of the entry barrier in antifoaming (when the drops are pre-emulsified). If the oil is placed on the top of the foam column (Figure 8A), several processes, such as oil spreading, oil solubilization, and evaporation (which could induce gradients in the surface tension and destabilization of the foam films) possibly play a significant role in the foam destruction. On the other hand, when the oil drops are pre-emulsified, the drop entry appears to be the critical step, which controls to a large extent the antifoam efficiency of the oil.[31] Indeed, the high entry barrier of silicone oil and *n*-C_{12}OH prevents the entry of emulsified oil drops, which explains why these oils do not cause a foam destruction after emulsification (viz. Figure 8B). For *n*-C_{12}OH, an additional problem is the negative equilibrium bridging coefficient. On the other side, the drops of 2BO and IHNP, possessing low entry barriers and positive bridging coefficients, easily destroy the foam by the mechanism illustrated in Figure 1.

The same solutions were tested again 1 week later to see how the solubilization of the oils affects their antifoam activity. The results were almost the same with one remarkable difference—the foam produced from the solution containing *n*-C_7OH was large (70 mL) and remained stable for the observation period of 1 h (Figure 8B). The microscope observations showed that *n*-C_7OH was solubilized in this aged solution, which explained why *n*-C_7OH had completely lost its antifoam activity. The other oils are less soluble and dispersed oil drops were observed in all of the remaining solutions, which is why the antifoam activity of these oils remained unaltered with time.

3.6.2. Foam Destruction by Pre-emulsified Oil Drops. The experiments described in this and the following subsections are performed by the Ross−Miles test. In Figure 9 and Table 3 we compare the antifoam activity of the oils at a concentration of 0.01 wt % (coarse emulsion). We first discuss the effect of the oils on the foam stability. The effect on the foamability of the solutions (which is far more complex for analysis) is discussed in section 3.6.4.

The results in Figure 9 show that only the drops of 2BO and IHNP are able to destroy the foam down to 40−50 mL for about 10 min. The foams produced in the presence of the other oils are very stable under these conditions. Note that the foam destruction pattern in the presence of 2BO and IHNP is very similar, though these two oils have very

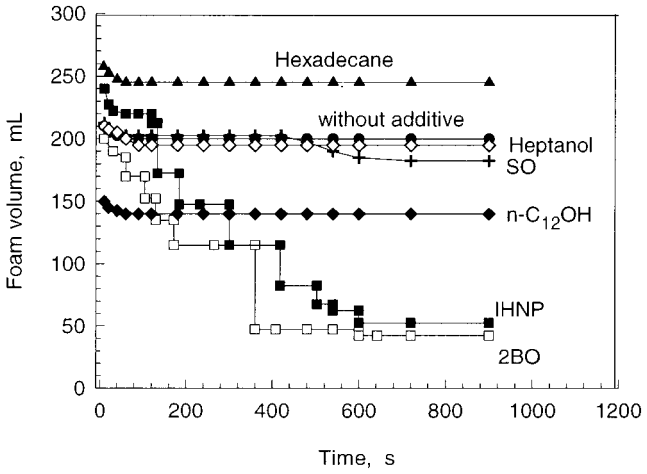

Figure 9. Comparison of the foamability and foam stability of 2.6 mM SDDBS solutions in the presence of 0.01 wt % of oily additive (coarse emulsion, Ross−Miles test).

Table 3. Initial, V_{IN}, and Final, V_F, Foam Volume in the Presence of 0.01 wt % of Oil (coarse emulsion)[a]

additive	V_{IN}, mL	V_F, mL	P_C^{CR}, Pa
no oil	210	200	
2BO	200	42	44
IHNP	240	52	73
n-C_{12}OH	150	140	>1500
n-C_7OH	210	195	*b*
SO	210	180	>3000
n-C16	260	245	≈400

[a] For comparison, the critical capillary pressure for drop entry, P_C^{CR}, is also shown. [b] Not measured.

different spreading behavior. This is another indication that the oil spreading has a secondary importance for the foam stability in these systems, while the bridging coefficients (should be positive) and the entry barrier (should be low) are more important. The lack of foam destruction by the drops of silicone oil is certainly due to its high entry barriers (Table 1). For *n*-C_{12}OH, the entry barrier and the equilibrium bridging coefficient are both unfavorable with respect to its antifoam activity. The heptanol is completely solubilized, so that no oil drops are present in the solution. Hexadecane also has no antifoam activity in the time scale of interest (15 min), though its bridging coefficient is positive. Additional experiments showed that the hexadecane indeed breaks the SDDBS foam, but the destruction process starts only after ca. 1 h (for comparison, the SDDBS foam in the absence of oil is very stable and no destruction is observed for more than 2 h). This delay is certainly due to the higher entry barrier of hexadecane (400 Pa)—more water should drain from the foam before the hexadecane drops can enter the walls of the GPBs and become active as antifoam entities.[6]

One interesting feature of the results shown in Figure 9 is the stepwise destruction of the foam column observed with IHNP- and 2BO-containing solutions. The foam is destroyed in steps of 10−20 mL (each step including hundreds of bubbles), separated by a relatively long periods, 1−2 min, without visible foam destruction. No such steps are seen in Figure 8A, where the oil is spread on the top of the foam column. Such a collective destruction of many bubbles in a single step can be explained by the mechanism illustrated in Figure 1.[6] The drainage of water from the foam column leads to a slow but steady narrowing of the Plateau borders and to an increase of the pressure that compresses the trapped oil drops. When the capillary pressure exceeds the critical value (the entry barrier) for one of the drops trapped in the upper layer of the foam column, the subsequent drop entry triggers an avalanche of film ruptures and drop entry events, so that the top portion of the foam column is destroyed. The visual observations show that the foam layer, which is destroyed in one step, roughly corresponds to the upper layer of dry foam (it appears more transparent in transmitted light than the remaining, wet part of the foam), which is formed as a result of the water drainage.

The residual foam, observed with 2BO- and IHNP-containing solutions (≈40 mL, corresponding to ≈4 cm height of the foam column), can be explained by the increased equilibrium cross section of the Plateau borders at low foam height, H. Equation 7 predicts that the minimal radius of the trapped sphere is $R_D \approx 11\ \mu$m for $H = 4$ cm. As explained in section 3.3, the main fraction of oil drops is of radius below 5 μm, and the larger drops are relatively rare. Hence, the probability for trapping oil drops, which are large enough to cause foam destruction, becomes rather small at low H. Furthermore, one sees from Figure 9 that the last steps in the foam decay curves become very small, i.e., the entry events do not lead to a massive destruction of bubbles in the upper layer of foam. The visual observations show that the last 40−50 mL of foam remains wet during the entire observation period, so that this foam is less vulnerable to destruction.

3.6.3. Experiments with Pre-equilibrated Solutions after Removal of the Oil Drops. As clarified by Kruglyakov et al.,[11−13] the antifoam activity of *n*-alkanols is primarily due to the emulsified oily drops. To check whether the same is true for 2BO and IHNP, we performed foam tests with pre-equilibrated solutions, from which the oil drops had been almost completely removed as explained in section 2.1. The tests showed that the removal of IHNP and 2BO drops lead to foams that were stable for a longer time (8−10 min). Afterward, a significant foam destruction was typically observed in one or two steps (down to $V_F \approx 80$ mL).

This result can be explained by taking into account the fact that some oil drops had remained in these solutions (it was impossible for us to remove completely all of the oil drops). Therefore, if a single big oil drop is trapped somewhere within the foam column, the entry of this drop could induce a mechanical shock that is powerful enough to destroy a big fraction of the foam (other oil drops were certainly captured in the foam as well).

It is worth noting that the foamability of solutions pre-equilibrated with 2BO was higher than that of pure SDDBS, while the foamability of the solutions pre-equilibrated with IHNP was lower. This observation is explained and discussed in the following subsection.

3.6.4. Effect of the Additive Concentration. The effect of the oil concentration was studied with *fine* emulsions of IHNP, 2BO, and *n*-C_7OH (Figure 10), because the reproducibility of the drop-size distribution was better when a rotor-stator homogenizer was used to disperse the oils.

In the absence of oil, the initial foam volume, V_{IN}, is about 205−210 mL and the final foam volume, V_F, is about 195−200 mL. The experiments with different oils show that V_F, which is determined mainly by the antifoam activity of the oil drops, is a monotonic function of the oil concentration; see Figure 10. For IHNP-containing solutions, V_F sharply decreases with the oil concentration down to 60 mL at 0.005 wt % and remains practically constant, $V_F \approx 40$−50 mL, at higher concentrations (0.01 to 0.05 wt %). Similarly, for 2BO solutions V_F drops to ≈60 mL at 0.005 wt % and remains almost constant at higher concentrations (Figure 10B). The final foam volume for

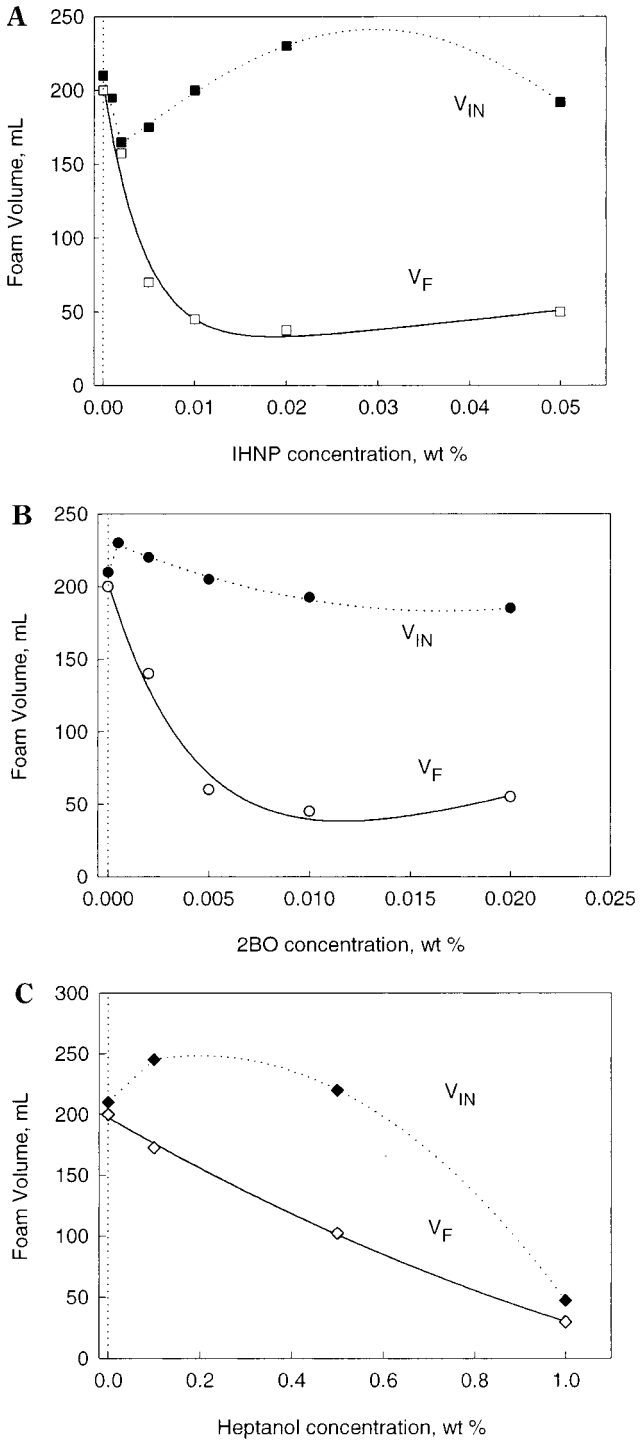

Figure 10. Effect of the oil concentration on the initial foam volume, V_{IN}, and the final foam volume, V_F: (A) IHNP; (B) 2BO; (C) *n*-C_7OH. The solutions contain 2.6 mM SDDBS, 12 mM NaCl, and oil dispersed by rotor-stator homogenizer (fine emulsion, Ross−Miles test).

n-C_7OH containing solutions is also a monotonically decreasing function of the alcohol concentration (Figure 10C). The comparison of the respective curves for these oils shows that 2BO and IHNP are active antifoams even at concentrations as low as 0.005 wt %, whereas more than 0.6 wt % of heptanol is needed for observing a significant antifoam activity.

Remarkably, the initial foam volume, V_{IN}, is a nonmonotonic function of the oil concentration: At IHNP concentration of 0.002 wt %, V_{IN} is substantially smaller (160 mL) but gradually increases with the oil concentration, $V_{IN} = 225$ mL at 0.02 wt %. The further increase of the oil concentration leads to reduction of the initial foam volume, $V_{IN} = 195$ mL at 0.05 wt %. These variations of V_{IN} are beyond the experimental error (±10 mL) and have been reproduced in several series of experiments.

Such a complex dependence of V_{IN} on the oil concentration can be explained by assuming that the presence of oil in the foaming solution leads to at least two opposite effects that are competing with each other: (1) a reduced DST, which facilitates the foam generation in the presence of oil, Figures 4 and 5, and (2) an antifoam effect of the oil droplets, which induce a coalescence of the newly created bubbles, and thereby suppress the foam generation.

On the basis of the DST results, one can suggest the following explanation of the observed dependence of V_{IN} on the IHNP concentration. At a very low oil concentration, the DST of the solutions is practically the same as that of the pure surfactant solution (Figure 5B). Therefore, the oil acts only as an antifoam (effect 2), decreasing the volume of the initially generated foam. At intermediate oil concentration (0.01−0.02 wt %), the coalescence of the oil drops with the solution surface during foaming leads to reduced DST (Figure 4) and to larger V_{IN} (effect 1 prevails). With the further increase of the oil concentration (0.05 wt %), the DST remains the same, while the bubble coalescence induced by oil drops becomes more intensive (effect 2 prevails) and less foam is generated.

The dependence of V_{IN} on the 2BO concentration seems simpler—V_{IN} decreases from 220 mL at 0.002 wt % down to 180 mL at 0.02 wt %. However, the foam tests with solutions, pre-equilibrated with 2BO and removed drops, have revealed that the drop removal results in a relatively high $V_{IN} \approx 230$ mL. These changes in V_{IN} are also larger than the experimental error and have been reproduced in several experimental series. These results can be explained by DST and by the antifoaming action of oil drops. The pre-equilibrated with 2BO solutions exhibit a reduced DST (Figure 5A) even in the absence of oil drops. Therefore, one may expect higher foamability of these solutions just as observed in the experiment (effect 1). The increase of the concentration of 2BO drops leads to enhanced coalescence of the foam bubbles during foaming and, hence, to a gradual decline of V_{IN} (effect 2 takes over).

As discussed above, heptanol is totally inactive as a foam breaker at 0.01 wt %, because it is rapidly solubilized in the surfactant micelles. The initial foam volume is increased in the presence of *n*-C_7OH at low concentrations, due to the reduced dynamic surface tension. One needs concentrations well above the solubility limit of 0.15 wt % to observe a substantial decrease of both V_{IN} and V_F. These results confirm the conclusion of Kruglyakov et al.[11−13] that the antifoam activity of *n*-C_7OH is primarily due to the presence of oily drops.

The comparison of the results from the foam tests with fine and coarse emulsions (cf. Figures 9 and 10) shows no big difference, in contrast to the large drop size effect observed in other systems.[6] This slight dependence of the foam stability on the size of IHNP and 2BO drops can be explained in the following way. In both types of emulsion (fine and coarse) we observe a significant number of large drops, which are able to destroy the foam after being compressed by the walls of the PBs (the entry barrier is very low for 2BO and IHNP). The stepwise transitions (presumably each of them induced by the entry of a single large drop), observed in the foam decay curves, show that several large drops are sufficient to trigger the observed process of foam destruction. In contrast, the systems studied in ref 6 did not show a stepwise foam destruction

pattern, which means that many drop entry events should take place for a significant foam destruction to occur. That is why the stability of the foams studied in ref 6 was strongly dependent on the mean drop size, while the upper boundary of the drop size distribution seems more important in the current systems.

4. Concluding Remarks

Foam tests and model experiments with several oils of different chemical structure are performed to clarify how these oils affect the foam stability and the foaminess of SDDBS solutions. The results show that the activity of these oils as foam breakers is determined mainly by their entry barrier (viz. by the stability of the asymmetric oil−water−air films) which should be low—otherwise the oil drops remain arrested in the Plateau borders during the process of foam drainage, without being able to destroy the foam. This is the main obstacle for silicone oil to be an active antifoam in SDDBS solution. For *n*-C_{12}OH the high entry barrier and the negative bridging coefficient are both unfavorable with respect to its antifoam activity. On the other side, oils having low entry barrier and positive entry coefficient (2BO and IHNP) demonstrate a significant antifoam activity.

No direct correlation between the spreading behavior of the oil (e.g., whether it spreads as a thin or thick layer on the solution surface, rate of oil spreading, or value of the spreading coefficient) and its foam breaking activity is observed. Two oils of rather different spreading behavior (2BO and IHNP) show similar antifoam activity, while *n*-C_{16} (whose spreading behavior is similar to that of 2BO) has no activity in the time scale of interest. On the other side, experiments described in refs 10 and 31 show that the presence of a spread oil layer (even a very thin one) on the surface of the foam film might reduce the entry barrier. Therefore, the oil spreading might facilitate to some extend the drop entry and the foam destruction, without being a crucial factor, however.

The effect of the oils on the foamability of the solutions is far more complex. The spreading oils are able to reduce the dynamic surface tension of the solutions, facilitating in this way the formation of a fresh surface. Hence, most of the oily additives enhance the foamability of the solutions at concentrations below and around the oil solubility limit (long-chain linear alcohols such as *n*-C_{12}OH might be exceptions for reasons discussed in ref 20). On the other hand, the emulsified oil drops induce a coalescence of the foam bubbles during the foam generation process and, as a result, the foamability of the solutions decreases at higher oil concentrations. Therefore, the dependence of the foamability of the surfactant solutions on the oil concentration is a nonmonotonic function and a careful examination of this dependence (in relation to the oil solubility limit) is needed before making any general conclusion about the effect of oil on the foaminess.

The foam tests confirmed the significant antifoam activity of *n*-C_7OH, but at a relatively high concentration (above 0.2 wt %) due to its high solubility in the surfactant solution. For comparison, 2BO (branched alkanol) and IHNP (branched ester) demonstrate a significant antifoam activity at concentrations as low as 0.005 wt %. Note that the *n*-C_{12}OH (linear alkanol of similar molecular mass) has no antifoam activity at this concentration. Therefore, the branched long-chain alkanols combine the advantages of long-chain *n*-alkanols (low solubility in the surfactant solutions) and medium-chain *n*-alkanols (low entry barrier). This makes the branched alkanols and other amphiphiles of similar molecular structure potentially applicable as antifoam agents.

Finally, let us note that the studied additives fall in the category of the so-called "slow antifoams",[6,39] which destroy the foam in the Plateau borders for a relatively long period of time (minutes or dozens of minutes). It has been well established[7,10,39] that the introduction of hydrophobic solid particles in the oils leads to formation of mixed oil−solid compounds, which often act as "fast antifoams", viz., they are much more active and destroy completely the foam within seconds. Recent experiments showed[10,39] that the fast antifoams break the foam films almost immediately after their formation. The main physicochemical characteristic, which determines whether a given antifoam would behave as a slow or fast one, is the entry barrier (for fast antifoams it is below ca. 20 Pa).

Acknowledgment. The support of this study by Colgate-Palmolive is gratefully acknowledged. The authors are indebted to Mrs. M. Temelska for the Ross−Miles tests, to Dr. S. Roussev and Mr. T. Argirov for the ellipsometrical measurements, and to Professor I. B. Ivanov and Professor P. A. Kralchevsky for the helpful discussions.

LA010600R